coatings

MDPI

Review

Preparation and Grafting Functionalization of Self-Assembled Chitin Nanofiber Film

Jun-ichi Kadokawa

Department of Chemistry, Biotechnology, and Chemical Engineering, Graduate School of Science and Engineering, Kagoshima University, 1-21-40 Korimoto, Kagoshima 890-0065, Japan; kadokawa@eng.kagoshima-u.ac.jp; Tel.: +81-99-285-7743

Academic Editor: Andriy Voronov
Received: 23 June 2016; Accepted: 8 July 2016; Published: 12 July 2016

Abstract: Chitin is a representative biomass resource comparable to cellulose. Although considerable efforts have been devoted to extend novel applications to chitin, lack of solubility in water and common organic solvents causes difficulties in improving its processability and functionality. Ionic liquids have paid much attention as solvents for polysaccharides. However, little has been reported regarding the dissolution of chitin with ionic liquids. The author found that an ionic liquid, 1-allyl-3-methylimidazolium bromide (AMIMBr), dissolved chitin in concentrations up to ~4.8 wt % and the higher contents of chitin with AMIMBr gave ion gels. When the ion gel was soaked in methanol for the regeneration of chitin, followed by sonication, a chitin nanofiber dispersion was obtained. Filtration of the dispersion was subsequently carried out to give a chitin nanofiber film. A chitin nanofiber/poly(vinyl alcohol) composite film was also obtained by co-regeneration approach. Chitin nanofiber-*graft*-synthetic polymer composite films were successfully prepared by surface-initiated graft polymerization technique. For example, the preparation of chitin nanofiber-*graft*-biodegradable polyester composite film was achieved by surface-initiated graft polymerization from the chitin nanofiber film. The similar procedure also gave chitin nanofiber-*graft*-polypeptide composite film. The surface-initiated graft atom transfer radical polymerization was conducted from a chitin macroinitiator film derived from the chitin nanofiber film.

Keywords: chitin; grafting; ion gel; nanofiber film; regeneration; self-assembly

1. Introduction

Polysaccharides are widely distributed in nature and exhibit important functions such as structural materials and energy providers [1,2]. Cellulose and chitin are the representative structural polysaccharides as the main components of cell wall in plants and of exoskeletons in crustaceans, shellfishes, and insects, respectively. Cellulose is composed of β(1→4)-linked D-glucose repeating units (Figure 1) [3]. Chitin has the similar structure as cellulose, but shows the difference in replacement of the hydroxy group in D-glucose units to the acetamido group at C-2 position (β(1→4)-linked *N*-acetyl-D-glucosamine repeating units) (Figure 1) [4–6]. These polysaccharides are the most abundant biomass resources on the earth, and accordingly, have been identified as eco-friendly and recyclable organic substances. Indeed, cellulose has practically been used in applications to furniture, clothes, foods, medicines, and so on. Compared with cellulose, chitin is still an unutilized biomass resource primary because of highly crystalline and bulk structure owing to numerous intra- and intermolecular hydrogen bonds, which cause the limitation of solubility with solvents [7]. Solubility problem of chitin is more serious compared with cellulose, leading to difficulty in practical application of chitin as functional materials.

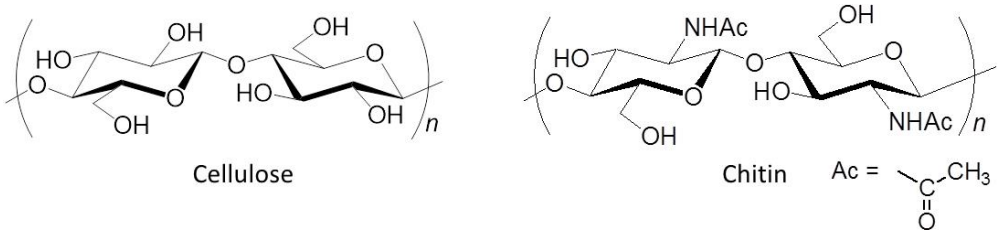

Figure 1. Chemical structures of cellulose and chitin.

Ionic liquids (ILs) have been identified as powerful solvents for polysaccharides [8–13]. ILs are low-melting-point molten salts, defined as those form liquids at ambient temperatures, e.g., lower than the boiling point of water [14,15]. The property is owing to that the liquid state is thermodynamically favorable because of large size and conformational flexibility of the ions, in which these behaviors give rise to small lattice enthalpies and large entropy changes that favor the liquid state [16]. A wide variety of chemical structures in ILs have been known by various combinations of organic cations, such as imidazolium, pyridinium, ammonium, and phosphonium, with inorganic and organic anions (Figure 2). Over the past decade, ILs have attracted much attention because of their specific characteristics such as an excellent thermal stability, a negligible vapor pressure, and controllable physical and chemical properties [17–19]. Beyond these traditional properties of ILs, interests and applications on ILs have been extended to the researches dealing with biological macromolecules such as naturally occurring polysaccharides [8–13], because ILs have been identified to specifically dissolve them.

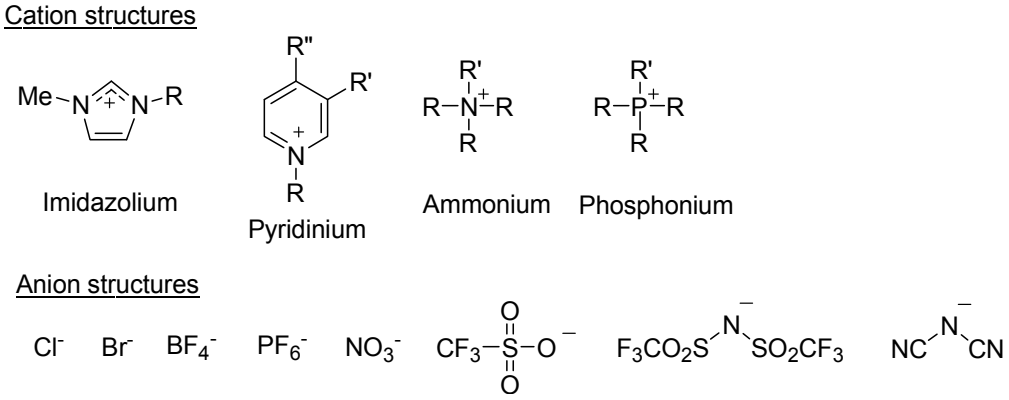

Figure 2. Typical cation and anion structures of ionic liquids (ILs).

In 1934, a molten *N*-ethylpyridinium chloride, in the presence of nitrogen-containing bases, has already been found to dissolve cellulose [20]. Although this study was probably the first example of the cellulose dissolution with IL-type solvents, it was considered to be of little practical value at the time because the concept of ILs had not been put forward. In 2002, an IL, 1-butyl-3-methylimidazolium chloride (BMIMCl, Figure 3), was found to dissolve cellulose in relatively high concentrations and this research opened up a new way for the development of a class of polysaccharide solvent systems [21]. Since this report was published, ILs have been used in the processing of cellulose and other polysaccharides, which mainly concern the dissolution, homogeneous derivatization and modification, and regeneration [8–13]. In contrast, only limited investigations have been reported regarding the dissolution of chitin with ILs [22–24]. So far, two types ILs, i.e., 1-allyl-3-methylimidazolium bromide (AMIMBr, Figure 3) and some imidazolium acetates with different substituents (1-allyl, 1-butyl, and 1-ethyl-3-methylimidazolium acetates, Figure 3) have been reported to dissolve chitin in several wt % concentrations [23,25–27]. The former IL, which was found to dissolve chitin by the author, is more stable than the latter ILs. Furthermore, AMIMBr can be prepared by a simple quaternarization reaction

of 1-methylimidazole with allyl bromide in high yield [28]. The dissolution of chitin with deep eutectic solvents (DESs), that is, ionic liquid analogues, composed of mixtures of choline halide-urea, chlorocholine chloride-urea, and choline chloride-thiourea were also investigated [29]. Consequently, maximum dissolution of chitin (9% w/w) was obtained in the choline chloride-thiourea system.

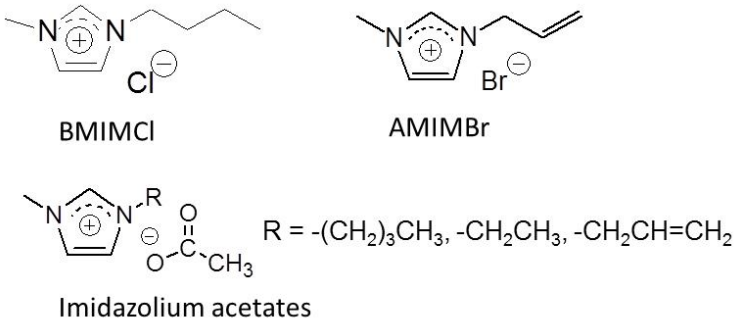

Figure 3. Representative ILs, which dissolve cellulose and chitin.

The author reported that AMIMBr dissolved a chitin powder from crab shells in concentrations up to ~4.8 wt %, and further formed ion gels with 6.5–10.7 wt % contents of chitin [26]. From the ion gel, chitin self-assembled into nanofibers by regeneration, which further formed a nanofiber film by entanglement [30–32]. Moreover, surface-initiated graft polymerization from the nanofiber film has been conducted to produce chitin nanofiber-*graft*-synthetic polymer composite materials [33]. In this review article, the comprehensive results on the preparation and grafting functionalization of the self-assembled chitin nanofiber film are presented.

2. Preparation of Self-Assembled Chitin Nanofiber Film from Ion Gel

The author reported that a clear solution of chitin (4.8 wt %) with AMIMBr was obtained by heating a mixture of a commercial chitin powder from crab shells with AMIMBr at 100 °C for 48 h (Figure 4) [26]. When mixtures of 6.5–10.7 wt % chitin with AMIMBr were left standing at room temperature for 24 h, heated at 100 °C for 48 h, and then cooled to room temperature, furthermore, they totally turned into the gel-like form (Figure 4). The dynamic rheological measurements showed that both 4.8 wt % and 6.5 wt % chitins with AMIMBr behaved as weak gels. However, the 6.5 wt % chitin with AMIMBr did not flow, while the 4.8 wt % chitin with AMIMBr started to flow upon leaning.

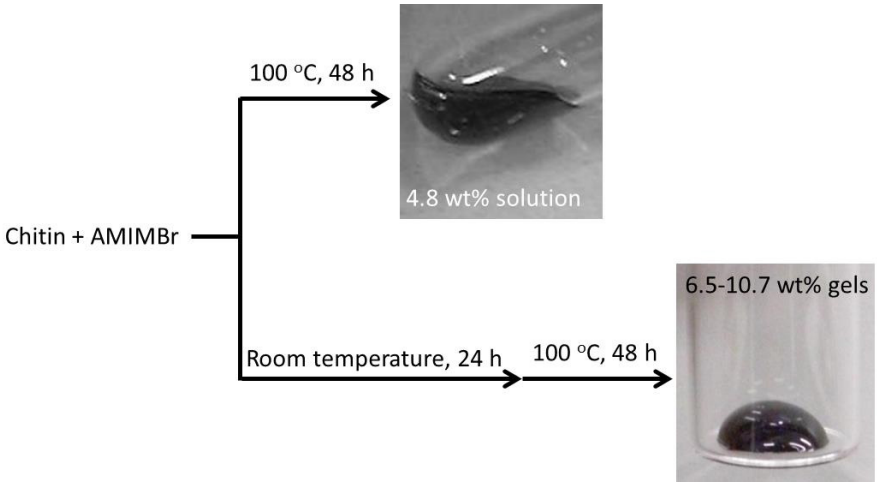

Figure 4. Dissolution (~4.8 wt %) and gelation (6.5–10.7 wt %) of chitin with 1-allyl-3-methylimidazolium bromide (AMIMBr).

The regeneration of chitin from the 9.1 wt %–10.7 wt % chitin ion gels with AMIMBr was carried out by soaking in methanol at room temperature for 24 h. The subsequent sonication gave dispersions of the regenerated chitin (Figure 5) [30]. The SEM image of the sample, which was prepared by dilution of the resulting dispersion, showed the nanofiber morphology with ca. 20–60 nm in width and several hundred nm in length (Figure 6a), indicating the self-assembling formation of the chitin nanofibers by the regeneration approach from the ion gels. When the resulting self-assembled nanofibers were isolated by filtration of the dispersion, a film was obtained (Figure 5). The SEM image of the resulting film exhibited the morphology of highly entangled nanofibers (Figure 6b). Such entangled structure from the nanofibers probably contributed to formation of the films.

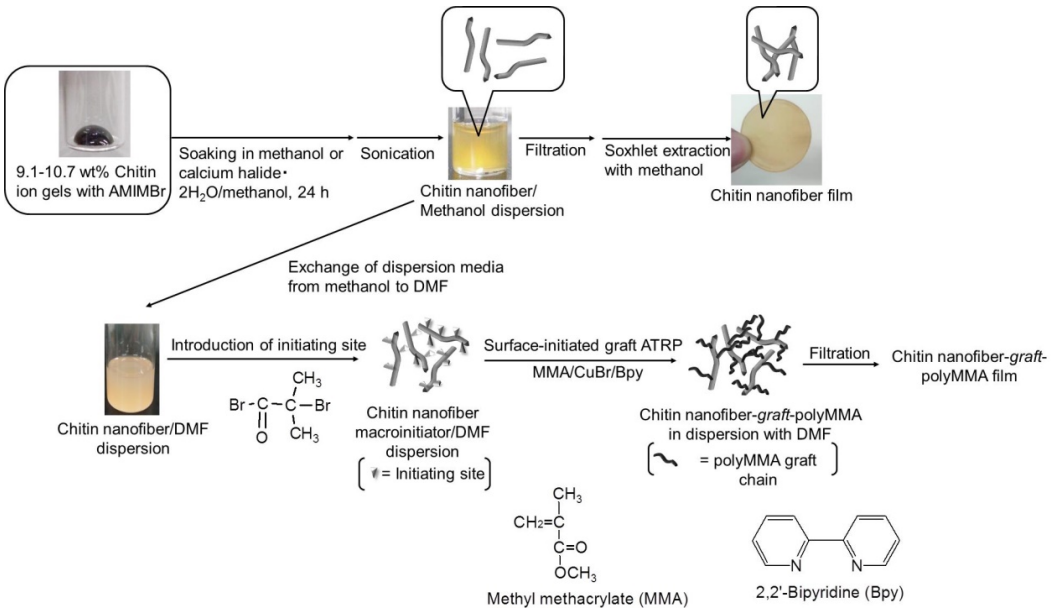

Figure 5. Preparation of self-assembled chitin nanofiber dispersion/film and preparation of chitin nanofiber macroinitiator dispersion and subsequent surface-initiated graft atom transfer radical polymerization (ATPR) of methyl methacrylate (MMA).

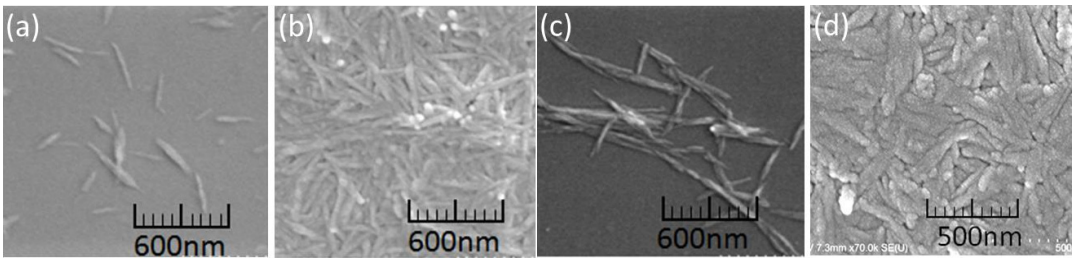

Figure 6. SEM images of chitin nanofiber dispersion and film obtained using methanol ((**a**) and (**b**), respectively), chitin nanofiber dispersion obtained using 0.765 mol/L $CaBr_2 \cdot 2H_2O$/methanol solution (**c**), and chitin nanofiber/PVA composite film (**d**).

Morphologies of self-assembled chitin nanofibers were changed when the regeneration from the ion gels were conducted using the several kinds of calcium halide$\cdot 2H_2O$/methanol solutions instead of a pure methanol [34]. The nanofiber assembly was not induced by the regeneration from the ion gel using $CaCl_2 \cdot 2H_2O$ and $CaBr_2 \cdot 2H_2O$/methanol solutions in high concentrations (3.06 mol/L and 1.53 mol/L, respectively), whereas the regeneration using $CaBr_2 \cdot 2H_2O$/methanol solution in lower concentration (0.765 mol/L) gave self-assembled nanofibers with higher aspect ratio as confirmed by the SEM image (Figure 6c). The tensile strength value of the film, which was obtained by filtration of the dispersion from such 0.765 mol/L $CaBr_2 \cdot 2H_2O$/methanol solution, was larger than that of the

films produced using the other methanol-based solutions. These results indicated that the mechanical properties were affected by morphologies of the chitin assemblies in the films.

Co-regeneration approach has been conducted to fabricate a self-assembled chitin nanofiber/poly(vinyl alcohol) (PVA) composite film (Figure 7) [30]. For the composite preparation, a solution of PVA (DP = ca. 4300) with a small amount of hot water was first mixed with the 9.1 wt % chitin ion gel with AMIMBr (feed weight ratio of chitin to PVA = 1:0.3). The co-regeneration of the two polymers was then conducted by soaking the mixture in methanol, because methanol is a poor solvent not only for chitin, but also for PVA. The resulting dispersion was subjected to filtration to isolate the regenerated polymeric materials, which were purified by Soxhlet extraction with methanol, to obtain the self-assembled chitin nanofiber/PVA composite film. The SEM image of the resulting composite film showed the nanofiber morphology (Figure 6d). This result suggested immiscibility of the two polymers in the composite. The PVA component probably filled in spaces among the fibers. The DSC result of the composite film suggested that PVA might partially be miscible at the interfacial area on the chitin nanofibers by hydrogen bonding between the two polymers. Both the tensile strength value and the elongation value at break of the composite film under tensile mode were larger than those of the self-assembled chitin nanofiber film. This result indicated reinforcing effect of PVA present in the chitin nanofiber film.

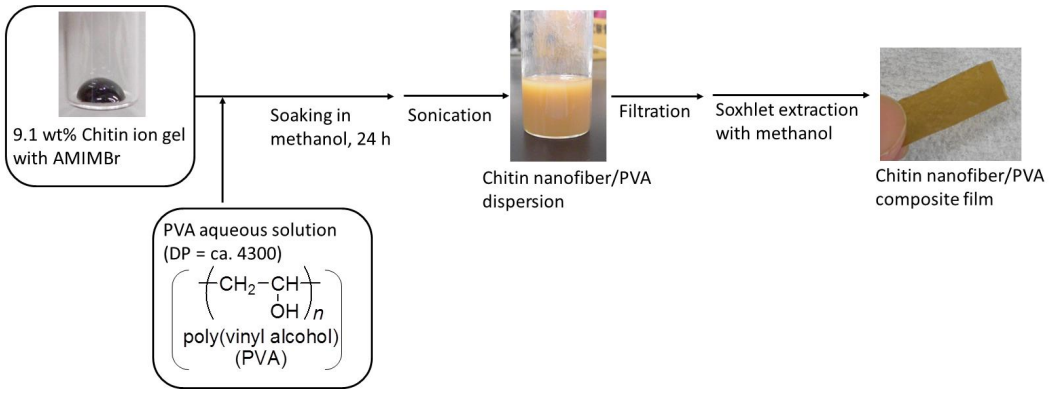

Figure 7. Preparation of chitin nanofiber/poly(vinyl alcohol) (PVA) composite film.

The self-assembled chitin nanofibers were also formed by gelation of chitin with the choline chloride-thiourea DES system (10% w/w) and subsequent dilution with water [35]. The resulting self-assembled chitin nanofibers were employed to prepare calcium alginate bio-nanocomposite gel beads [35].

3. Surface-Initiated Graft Polymerization from Self-Assembled Chitin Nanofiber Film

Surface-initiated graft polymerization of cyclic and vinyl monomers from the self-assembled chitin nanofiber film has been conducted to fabricate composite materials [33]. Such composites can be expected to exhibit specific functions such as influence of interfacial adhesion on mechanical properties [36–38]. For example, surface-initiated ring-opening graft copolymerization of L-lactide (LA)/ε-caprolactone (CL) monomers initiated from hydroxy groups on the self-assembled chitin nanofiber was attempted in the presence of tin(II) 2-ethylhexanoate as a Lewis acid catalyst to produce chitin nanofiber-*graft*-poly(LA-*co*-CL) film (Figure 8) [39]; poly(LA-*co*-CL) is a well-known biodegradable polyester [40,41] and can be synthesized by ring-opening copolymerization of LA/CL monomers initiated by alcohols [42,43]. To efficiently take place the ring-opening graft copolymerization of LA/CL on surface of the nanofibers, spaces among the fibers were made by immersing the film in water for 10 s. Then, the surface-initiated ring-opening graft copolymerization of LA/CL (feed molar ratio = 10:90) from the pre-treated film was conducted as follows. After the film was immersed in a solution of LA/CL in toluene, tin(II) 2-ethylhexanoate (ca. 5 mol% for the

monomers), was added and the mixture was heated at 80 °C for 48 h to occur the ring-opening copolymerization. The IR spectrum of the resulting film exhibited carbonyl absorption at 1739 cm^{-1} due to the ester linkage of poly(LA-*co*-CL), suggesting the presence of poly(LA-*co*-CL) in the product, which was explanatorily bound to the nanofibers by covalent linkage. The LA/CL unit ratio (30/70) in the polyester, which was determined by ^{1}H NMR analysis, was higher than that in feed (10/90) because of the higher reactivity of LA than CL in the copolymerization [44]. The SEM image of the resulting film indicated increase of the fiber widths (60–100 nm) compared with those of the original pre-treated film and some fibers were merged at the interfacial areas, that was probably caused by the grafted polyesters present on the nanofibers (Figure 9a). The stress-strain curve of the resulting film under tensile mode exhibited the larger elongation value (7.2%) at break than that of the original pre-treated chitin nanofiber film (1.1%) (Figure 10). When the surface-initiated ring-opening graft copolymerization of LA/CL was conducted in various monomer feed ratios, the grafting amounts of poly(LA-*co*-CL)s on the nanofibers increased with increasing the LA/CL feed molar ratios.

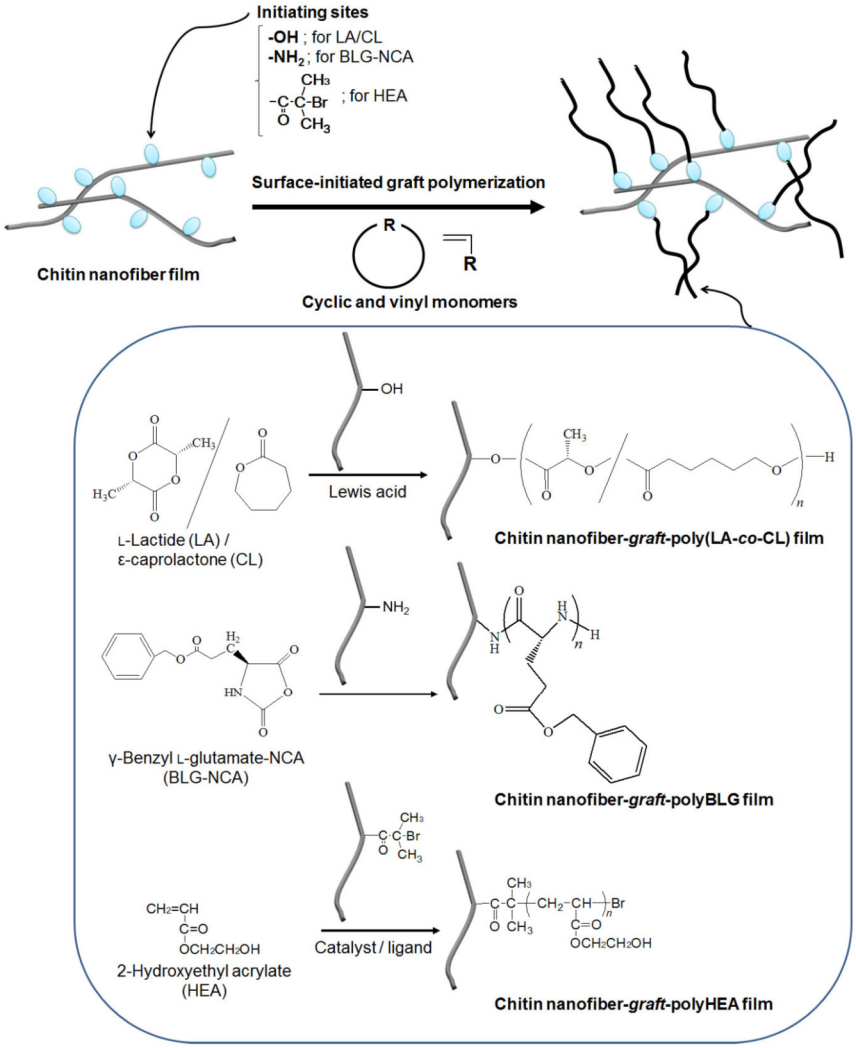

Figure 8. Surface-initiated graft (*co*)polymerization of L-lactide (LA)/ε-caprolactone (CL), γ-benzyl L-glutamate-*N*-carboxyanhydride (BLG-NCA), and 2-hydroxyethyl acrylate (HEA) from chitin nanofiber films with appropriate initiating sites.

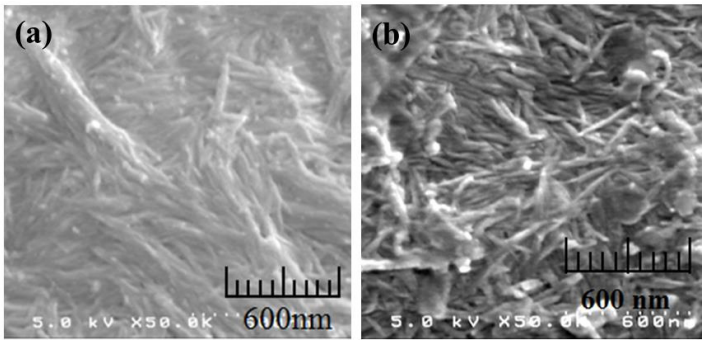

Figure 9. SEM images of chitin nanofiber-*graft*-poly(LA-*co*-CL) film (**a**) and chitin nanofiber-*graft*-polyBLG film (**b**).

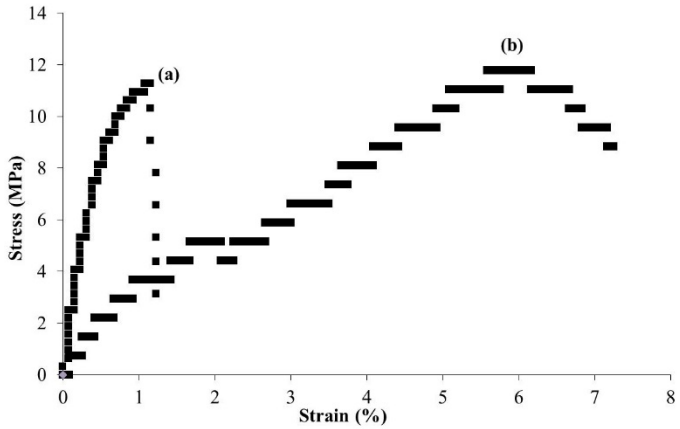

Figure 10. Stress-strain curves of pre-treated chitin nanofiber film (**a**) and chitin nanofiber-*graft*-poly(LA-*co*-CL) film (**b**).

Chitin nanofiber-*graft*-synthetic polypeptide film was also fabricated by surface-initiated polymerization approach. Because synthetic polypeptides with well-defined structure are synthesized by ring-opening polymerization of α-amino acid *N*-carboxyanhydrides (NCAs) accompanied with decarboxylation initiated by amino groups [45,46], the surface-initiated graft polymerization of a NCA monomer from the self-assembled chitin nanofiber film having amino initiating groups was performed [47]. As the NCA monomer, γ-benzyl L-glutamate-NCA (BLG-NCA) was particularly selected because its ring-opening polymerization and subsequent hydrolysis of benzyl ester gives poly(L-glutamic acid) having carboxylic acid functional groups (Figure 8). Partial deacetylation of acetamido groups in the chitin nanofiber film was conducted by the treatment with 40% (w/v) NaOH aq. at 80 °C for 7 h [48] to generate amino initiating groups on the nanofibers (degree of deacetylation = 24%). The resulting partially deacetylated chitin nanofiber film was immersed in a solution of BLG-NCA (20 equiv. with an amino group) in ethyl acetate at 0 °C for 24 h to take place the surface-initiated graft polymerization from amino groups. The IR spectrum of the product showed C=O absorption due to ester linkage at 1735 cm^{-1}, strongly suggesting the presence of polyBLG in the product, which was explanatorily bound to the nanofibers by covalent linkage. The grafting amount of the polyBLG chains was evaluated by the weight difference of the films before and after the graft polymerization to be 18 wt %. The SEM image of the produced film observed nanofiber morphology, but some fibers were merged at the interfacial areas, that was probably caused by the grafted polyBLG chains present on the nanofibers (Figure 9b).

A highly flexible chitin nanofiber-*graft*-poly(L-glutamic acid sodium salt) (chitin nanofiber-*graft*-polyLGA) network film was obtained by alkaline hydrolysis of ester linkages in the polyBLG chains to generate the polyLGA chains, followed by condensation of the produced sodium carboxylate groups with amino groups present in the film (Figure 11). The chitin nanofiber-*graft*-polyBLG film was first

immersed in 1.0 mol/L NaOH aq. at 60 °C for 5 h for the alkaline hydrolysis of benzyl esters to obtain the chitin nanofiber-*graft*-polyLGA film having sodium carboxylate groups. The IR spectrum of the film after the alkaline treatment supported that benzyl esters were completely hydrolyzed to generate sodium carboxylate groups. The condensation of the generated carboxylate groups with amino groups present at the terminal end of the polyLGA chains or the remaining amino groups present on the nanofibers, which did not induce the initiation of the graft polymerization, was then conducted using the *N*-hydroxysuccinimide/ 1-ethyl-3-(3-dimethylaminopropyl)carbodiimide (NHS/EDC) condensing agent (10 equiv. with a carboxylate group) in water at room temperature for 12 h to construct polyLGA or polyLGA/chitin networks in the film. The stress-strain curve of the chitin nanofiber-*graft*-polyBLG film under tensile mode showed the lager elongation value at break than that of the chitin nanofiber film with the comparable tensile strength values. This result suggested the more elastic nature of the chitin nanofiber-*graft*-polyBLG film. The stress-strain curve of the chitin nanofiber-*graft*-polyLGA network film exhibited the larger values both in tensile strength and elongation at break than those of the chitin nanofiber and chitin nanofiber-*graft*-polyBLG films. These data indicated the superior mechanical property of the chitin nanofiber-*graft*-polyLGA network film as this showed the highly flexible nature and was bended without breaking.

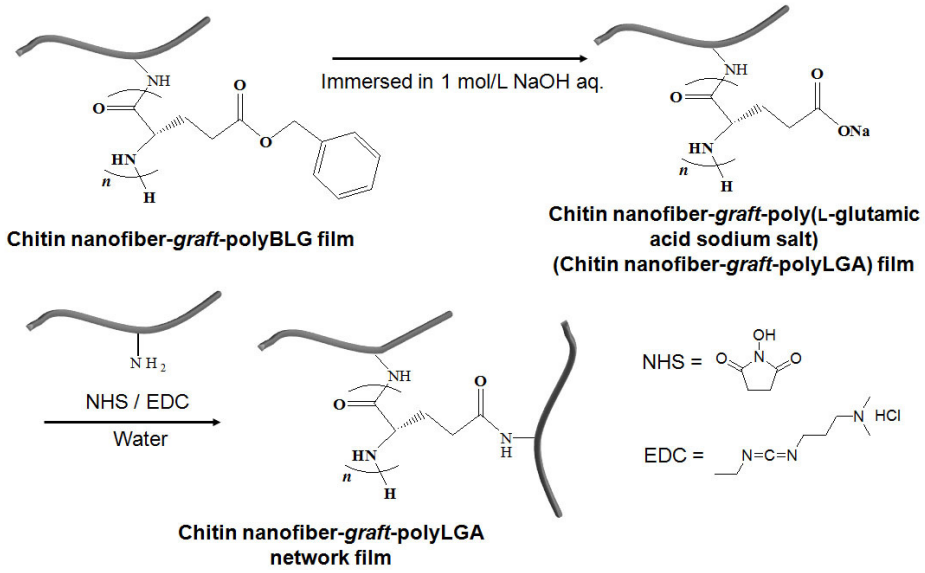

Figure 11. Alkaline treatment of chitin nanofiber-*graft*-polyBLG film and subsequent condensation to produce chitin nanofiber-*graft*-polyLGA network film.

Surface-initiated graft atom transfer radical polymerization (ATRP) from a chitin nanofiber macroinitiator film was also investigated. ATRP is one of the facile and versatile living radical polymerization techniques and has been employed to synthesize a wide range of polymeric materials with well-defined structure [49,50]. Because of the fact that ATRP can be initiated by α-haloalkylacyl groups, the chitin nanofiber macroinitiator film with the initiating groups was provided by esterification of the hydroxy groups on the self-assembled chitin nanofibers with α-bromoisobutyryl bromide (Figure 12) [51,52]. The degree of substitution of α-bromoisobutyrate groups on the chitin nanofiber film surface was calculated by SEM-EDX measurement to be 0.61. The surface-initiated ATRP of 2-hydroxyethyl acrylate (HEA) (20 equiv. with an initiating site) from the macroinitiator film was then examined in the presence of CuBr (catalyst)/2,2′-bipyridine (Bpy, ligand) in 3 wt % LiCl/DMAc at 60 °C to produce chitin nanofiber-*graft*-polyHEA films (Figure 12) [52]. The intensity ratio of the ester C=O absorption to the amido C=O absorption in the IR spectra of the products increased compared with those of the macroinitiator film, indicating the progress of the graft polymerization. The conversions of HEA increased with increasing reaction times. For gel permeation chromatography (GPC) analysis of the resulting polyHEAs, the graft chains were cleaved from the composite films by alkaline

hydrolysis to yield poly(acrylic acid)s, which were then converted into poly(methyl acrylate)s by methyl esterification. The GPC peaks of the resulting poly(methyl acrylate)s shifted to higher molecular weight regions with increasing reaction times. These results strongly supported that the longer polyHEA chains were generated on the chitin nanofibers by a gradual ATRP process with prolonged reaction times. The SEM image of chitin nanofiber-*graft*-polyHEA film yielded from the lower monomer conversion (6%, polymerization time 3 h) showed nanofiber morphology with the increased fiber width compared with that of the macroinitiator film (20 and 40 nm, (Figure 13a,b) respectively). The SEM image of chitin nanofiber-*graft*-polyHEA film with a higher monomer conversion (71%, polymerization time 24 h), on the other hand, did not observe the nanofiber morphology (Figure 13c), probably because that the nanofibers were totally covered by the longer graft polyHEA chains. The stress-strain curves of the chitin nanofiber-*graft*-polyHEA films under tensile mode showed the larger elongation values at break compared with the original chitin nanofiber film. Moreover, the values increased with increasing monomer conversions, while the tensile strength values decreased. These data indicated the enhancement of flexibility by grafting the longer polyHEA chains on the chitin nanofiber film.

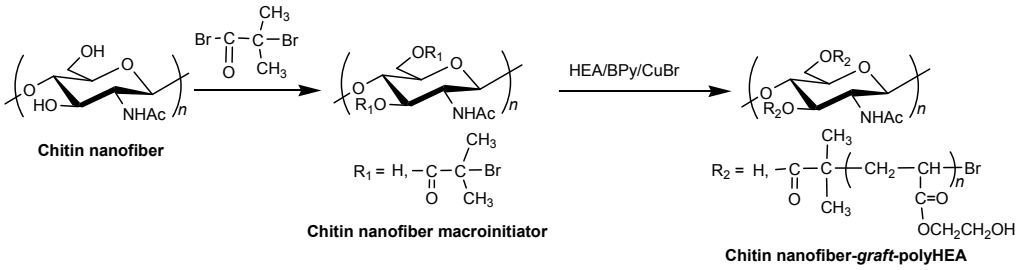

Figure 12. Preparation of chitin nanofiber macroinitiator film and subsequent surface-initiated graft atom transfer radical polymerization (ATRP) of HEA.

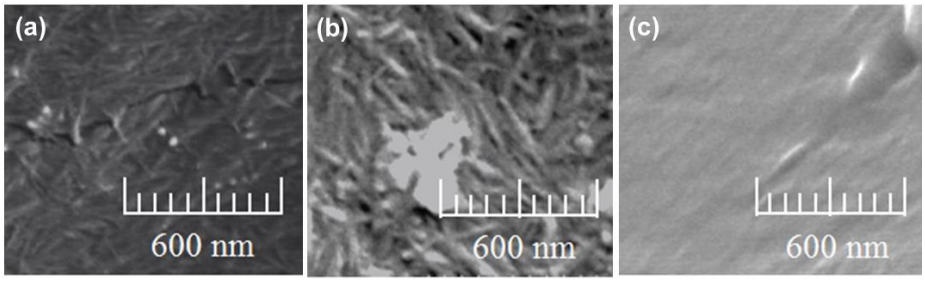

Figure 13. SEM images of chitin nanofiber macroinitiator film (**a**) and chitin nanofiber-*graft*-polyHEA films obtained by the reaction times of 3 and 24 h ((**b**) and (**c**), respectively).

Surface-initiated graft ATRP of methyl methacrylate (MMA) on the chitin nanofibers under dispersion conditions was investigated, followed by entanglement of the products to fabricate chitin nanofiber-*graft*-polyMMA films with nanofiber morphology (Figure 5) [53]. For graft ATRP on the self-assembled chitin nanofibers under dispersion conditions, the reaction of α-bromoisobutyryl bromide with hydroxy groups on the chitin nanofibers was conducted in the dispersion to produce the macroinitiator in-situ. Because the large amounts of methanol present in the dispersion potentially react with α-bromoisobutyryl bromide, exchange of dispersion medium from methanol to other liquids that did not react with α-bromoisobutyryl bromide was attempted. Consequently, the exchange to *N*,*N*-dimethylformamide (DMF) with retaining dispersion state was achieved. Accordingly, the reaction of α-bromoisobutyryl bromide (20 equiv. with a repeating unit of chitin) with hydroxy groups on the chitin nanofibers in the DMF dispersion was carried out in the presence of pyridine to give the chitin nanofiber macroinitiators. The SEM image of the resulting dispersion showed the nanofiber morphology. From the intensity ratio of the ester C=O absorption to the amido C=O absorption in the IR spectrum of the product, the functionality of the initiating sites on chitin nanofibers was estimated to be 0.37 with a repeating unit of chitin. Surface-initiated graft ATRP of MMA (5 or 10 equiv.

with an initiating site) on the resulting chitin nanofiber macroinitiators was then performed using CuBr and Bpy in the dispersion with DMF at 60 °C for 24 h. The resulting materials were isolated from the dispersion by filtration, which formed films. The intensities of the carbonyl absorptions due to ester linkage in the IR spectra of the products was higher than those of the chitin nanofiber macroinitiators, indicating the progress of the graft polymerization. Moreover, the intensity ratios in IR spectra also suggested the generation of the longer graft chains using 10 equiv. of MMA than using 5 equiv. The SEM images of the resulting films observed the nanofiber morphologies, which were further merged at interfacial areas (Figure 14). The SEM image of the aforementioned chitin nanofiber-*graft*-polyHEA film with the longer graft chains, which was produced by surface-initiated graft ATRP on the film, did not show nanofiber morphology (Figure 13c). In the surface-initiated graft ATRP under dispersion conditions, on the other hand, the polymerization occurred on the surfaces of individual nanofibers. Then, the nanofibers were entangled during filtration and merged among the non-crystalline polyMMA graft chains on the nanofibers.

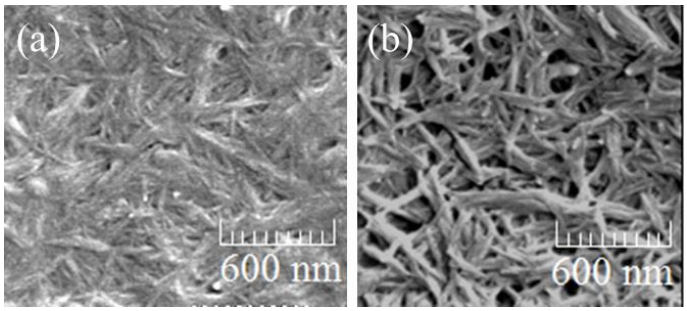

Figure 14. SEM images of chitin nanofiber-*graft*-polyMMA film ((**a**) MMA 5 equiv. and (**b**) MMA 10 equiv.).

4. Conclusions

Based on the fact that AMIMBr formed a chitin ion gel, the self-assembled chitin nanofiber film was easily fabricated by the regeneration from the gel using methanol, followed by sonication and filtration. The highly entanglement from the nanofibers during the process contributed to formation the film. The co-regeneration approach from the ion gel achieved to produce the chitin nanofiber/PVA composite film. The surface-initiated graft polymerization technique from the chitin nanofiber film was conducted to obtain the composite films with polyester, polypeptide, and poly(meth)acrylates. The present approaches provide the efficient use of the representative biomass, chitin to fabricate the nanofiber film, which further convert into composite films with synthetic polymers. These chitin-based nanofiber films have a potential to be employed as practical materials in biomedical, tissue engineering, and environmentally benign fields in the future.

Acknowledgments: The author is indebted to the co-workers, whose names are found in references from his papers, for their enthusiastic collaborations.

Conflicts of Interest: The author declares no conflict of interest.

References

1. Schuerch, C. Polysaccharides. In *Encyclopedia of Polymer Science and Engineering*, 2nd ed.; Mark, H.F., Bilkales, N., Overberger, C.G., Eds.; John Wiley & Sons: New York, NY, USA, 1986; Volume 13, pp. 87–162.
2. Berg, J.M.; Tymoczko, J.L.; Stryer, L. *Biochemistry*, 7th ed.; W.H. Freeman: New York, NY, USA, 2012.
3. Klemm, D.; Heublein, B.; Fink, H.P.; Bohn, A. Cellulose: Fascinating biopolymer and sustainable raw material. *Angew. Chem. Int. Ed.* **2005**, *44*, 3358–3393. [CrossRef] [PubMed]
4. Kurita, K. Chitin and chitosan: Functional biopolymers from marine crustaceans. *Mar. Biotechnol.* **2006**, *8*, 203–226. [CrossRef] [PubMed]
5. Rinaudo, M. Chitin and chitosan: Properties and applications. *Prog. Polym. Sci.* **2006**, *31*, 603–632. [CrossRef]

6. Pillai, C.K.S.; Paul, W.; Sharma, C.P. Chitin and chitosan polymers: Chemistry, solubility and fiber formation. *Prog. Polym. Sci.* **2009**, *34*, 641–678. [CrossRef]
7. Muzzarelli, R.A.A. Biomedical exploitation of chitin and chitosan via mechano-chemical disassembly, electrospinning, dissolution in imidazolium ionic liquids, and supercritical drying. *Mar. Drugs* **2011**, *9*, 1510–1533. [CrossRef] [PubMed]
8. El Seoud, O.A.; Koschella, A.; Fidale, L.C.; Dorn, S.; Heinze, T. Applications of ionic liquids in carbohydrate chemistry: A window of opportunities. *Biomacromolecules* **2007**, *8*, 2629–2647. [CrossRef] [PubMed]
9. Liebert, T.; Heinze, T. Interaction of ionic liquids with polysaccharides 5. Solvents and reaction media for the modification of cellulose. *Bioresources* **2008**, *3*, 576–601.
10. Feng, L.; Chen, Z.I. Research progress on dissolution and functional modification of cellulose in ionic liquids. *J. Mol. Liq.* **2008**, *142*, 1–5. [CrossRef]
11. Pinkert, A.; Marsh, K.N.; Pang, S.S.; Staiger, M.P. Ionic liquids and their interaction with cellulose. *Chem. Rev.* **2009**, *109*, 6712–6728. [CrossRef] [PubMed]
12. Gericke, M.; Fardim, P.; Heinze, T. Ionic liquids—Promising but challenging solvents for homogeneous derivatization of cellulose. *Molecules* **2012**, *17*, 7458–7502. [CrossRef] [PubMed]
13. Isik, M.; Sardon, H.; Mecerreyes, D. Ionic liquids and cellulose: Dissolution, chemical modification and preparation of new cellulosic materials. *Int. J. Mol. Sci.* **2014**, *15*, 11922–11940. [CrossRef] [PubMed]
14. Welton, T. Room-temperature ionic liquids. Solvents for synthesis and catalysis. *Chem. Rev.* **1999**, *99*, 2071–2083. [CrossRef] [PubMed]
15. Hallett, J.P.; Welton, T. Room-temperature ionic liquids: Solvents for synthesis and catalysis. 2. *Chem. Rev.* **2011**, *111*, 3508–3576. [CrossRef] [PubMed]
16. Wasserscheid, P.; Keim, W. Ionic liquids—New "solutions" for transition metal catalysis. *Angew. Chem. Int. Ed.* **2000**, *39*, 3772–3789.
17. Davis, J.H. Task-specific ionic liquids. *Chem. Lett.* **2004**, *33*, 1072–1077. [CrossRef]
18. Lee, S.G. Functionalized imidazolium salts for task-specific ionic liquids and their applications. *Chem. Commun.* **2006**, 1049–1063. [CrossRef] [PubMed]
19. Giernoth, R. Task-specific ionic liquids. *Angew. Chem. Int. Ed.* **2010**, *49*, 2834–2839. [CrossRef] [PubMed]
20. Graenacher, C. Cellulose solution. US Patent 1943176, 1934.
21. Swatloski, R.P.; Spear, S.K.; Holbrey, J.D.; Rogers, R.D. Dissolution of cellose with ionic liquids. *J. Am. Chem. Soc.* **2002**, *124*, 4974–4975. [CrossRef] [PubMed]
22. Zakrzewska, M.E.; Bogel-Łukasik, E.; Bogel-Łukasik, R. Solubility of carbohydrates in ionic liquids. *Energy Fuels* **2010**, *24*, 737–745. [CrossRef]
23. Wang, W.T.; Zhu, J.; Wang, X.L.; Huang, Y.; Wang, Y.Z. Dissolution behavior of chitin in ionic liquids. *J. Macromol. Sci. Part B Phys.* **2010**, *49*, 528–541. [CrossRef]
24. Jaworska, M.M.; Kozlecki, T.; Gorak, A. Review of the application of ionic liquids as solvents for chitin. *J. Polym. Eng.* **2012**, *32*, 67–69. [CrossRef]
25. Wu, Y.; Sasaki, T.; Irie, S.; Sakurai, K. A novel biomass-ionic liquid platform for the utilization of native chitin. *Polymer* **2008**, *49*, 2321–2327. [CrossRef]
26. Prasad, K.; Murakami, M.; Kaneko, Y.; Takada, A.; Nakamura, Y.; Kadokawa, J. Weak gel of chitin with ionic liquid, 1-allyl-3-methylimidazolium bromide. *Int. J. Biol. Macromol.* **2009**, *45*, 221–225. [CrossRef] [PubMed]
27. Qin, Y.; Lu, X.M.; Sun, N.; Rogers, R.D. Dissolution or extraction of crustacean shells using ionic liquids to obtain high molecular weight purified chitin and direct production of chitin films and fibers. *Green Chem.* **2010**, *12*, 968–971. [CrossRef]
28. Zhao, D.B.; Fei, Z.F.; Geldbach, T.J.; Scopelliti, R.; Laurenczy, G.; Dyson, P.J. Allyl-functionalised ionic liquids: Synthesis, characterisation, and reactivity. *Helv. Chim. Acta* **2005**, *88*, 665–675. [CrossRef]
29. Sharma, M.; Mukesh, C.; Mondal, D.; Prasad, K. Dissolution of a-chitin in deep eutectic solvents. *RSC Adv.* **2013**, *3*, 18149–18155. [CrossRef]
30. Kadokawa, J.; Takegawa, A.; Mine, S.; Prasad, K. Preparation of chitin nanowhiskers using an ionic liquid and their composite materials with poly(vinyl alcohol). *Carbohydr. Polym.* **2011**, *84*, 1408–1412. [CrossRef]
31. Kadokawa, J. Ionic liquid as useful media for dissolution, derivatization, and nanomaterial processing of chitin. *Green Sustain. Chem.* **2013**, *3*, 19–25. [CrossRef]

32. Takada, A.; Kadokawa, J. Fabrication and characterization of polysaccharide ion gels with ionic liquids and their further conversion into value-added sustainable materials. *Biomolecules* **2015**, *5*, 244–262. [CrossRef] [PubMed]
33. Kadokawa, J. Fabrication of nanostructured and microstructured chitin materials through gelation with suitable dispersion media. *RSC Adv.* **2015**, *5*, 12736–12746. [CrossRef]
34. Tajiri, R.; Setoguchi, T.; Wakizono, S.; Yamamoto, K.; Kadokawa, J. Preparation of self-assembled chitin nanofibers by regeneration from ion gels using calcium halide· dihydrate/methanol solutions. *J. Biobased Mater. Bioenergy* **2013**, *7*, 655–659. [CrossRef]
35. Mukesh, C.; Mondal, D.; Sharma, M.; Prasad, K. Choline chloride-thiourea, a deep eutectic solvent for the production of chitin nanofibers. *Carbohydr. Polym.* **2014**, *103*, 466–471. [CrossRef] [PubMed]
36. Felix, J.M.; Gatenholm, P. The nature of adhesion in composites of modified cellulose fibers and polypropylene. *J. Appl. Polym. Sci.* **1991**, *42*, 609–620. [CrossRef]
37. Valadez-Gonzalez, A.; Cervantes-Uc, J.M.; Olayo, R.; Herrera-Franco, P.J. Effect of fiber surface treatment on the fiber–matrix bond strength of natural fiber reinforced composites. *Compos. Part B Eng.* **1999**, *30*, 309–320. [CrossRef]
38. Vautard, F.; Fioux, P.; Vidal, L.; Schultz, J.; Nardin, M.; Defoort, B. Influence of the carbon fiber surface properties on interfacial adhesion in carbon fiber–acrylate composites cured by electron beam. *Compos. Part A Appl. Sci. Manuf.* **2011**, *42*, 859–867. [CrossRef]
39. Setoguchi, T.; Yamamoto, K.; Kadokawa, J. Preparation of chitin nanofiber-*graft*-poly(L-lactide-*co*-e-caprolactone) films by surface-initiated ring-opening graft copolymerization. *Polymer* **2012**, *53*, 4977–4982. [CrossRef]
40. Albertsson, A.C.; Varma, I.K. Aliphatic polyesters: Synthesis, properties and applications. *Adv. Polym. Sci.* **2002**, *157*, 1–40.
41. Seyednejad, H.; Ghassemi, A.H.; van Nostrum, C.F.; Vermonden, T.; Hennink, W.E. Functional aliphatic polyesters for biomedical and pharmaceutical applications. *J. Control. Release* **2011**, *152*, 168–176. [CrossRef] [PubMed]
42. Lou, X.D.; Detrembleur, C.; Jérôme, R. Novel aliphatic polyesters based on functional cyclic (di)esters. *Macromol. Rapid Commun.* **2003**, *24*, 161–172. [CrossRef]
43. Jérôme, C.; Lecomte, P. Recent advances in the synthesis of aliphatic polyesters by ring-opening polymerization. *Adv. Drug Deliv. Rev.* **2008**, *60*, 1056–1076. [CrossRef] [PubMed]
44. Grijpma, D.W.; Pennings, A.J. Polymerization temperature effects on the properties of L-lactide and e-caprolactone copolymers. *Polym. Bull.* **1991**, *25*, 335–341. [CrossRef]
45. Kricheldorf, H.R. Polypeptides and 100 years of chemistry of alpha-amino acid *N*-carboxyanhydrides. *Angew. Chem. Int. Ed.* **2006**, *45*, 5752–5784. [CrossRef] [PubMed]
46. Deming, T.J. Synthetic polypeptides for biomedical applications. *Prog. Polym. Sci.* **2007**, *32*, 858–875. [CrossRef]
47. Kadokawa, J.; Setoguchi, T.; Yamamoto, K. Preparation of highly flexible chitin nanofiber-*graft*-poly(g-L-glutamic acid) network film. *Polym. Bull.* **2013**, *70*, 3279–3289. [CrossRef]
48. Phongying, S.; Aiba, S.; Chirachanchai, S. Direct chitosan nanoscaffold formation via chitin whiskers. *Polymer* **2007**, *48*, 393–400. [CrossRef]
49. Kamigaito, M.; Ando, T.; Sawamoto, M. Metal-catalyzed living radical polymerization. *Chem. Rev.* **2001**, *101*, 3689–3745. [CrossRef] [PubMed]
50. Matyjaszewski, K. Atom transfer radical polymerization (ATRP): Current status and future perspectives. *Macromolecules* **2012**, *45*, 4015–4039. [CrossRef]
51. Yamamoto, K.; Yoshida, S.; Mine, S.; Kadokawa, J. Synthesis of chitin-*graft*-polystyrene via atom transfer radical polymerization initiated from a chitin macroinitiator. *Polym. Chem.* **2013**, *4*, 3384–3389. [CrossRef]
52. Yamamoto, K.; Yoshida, S.; Kadokawa, J. Surface-initiated atom transfer radical polymerization from chitin nanofiber macroinitiator film. *Carbohydr. Polym.* **2014**, *112*, 119–124. [CrossRef] [PubMed]
53. Endo, R.; Yamamoto, K.; Kadokawa, J. Surface-initiated graft atom transfer radical polymerization of methyl methacrylate from chitin nanofiber macroinitiator under dispersion conditions. *Fibers* **2015**, *3*, 338–347. [CrossRef]